Research Article | Vol. 33, No. 20 / 6 Oct 2025 / Optics Express 43036

Optics EXPRESS

Ultra-stretchable elastomeric suspended-core optical fibers for wearable sensing applications

XIANGYU YAN,[1,†] CHEN CHEN,[1,†] ZHENCHENG LI,[1] YANG LUO,[1] CHANG LIU,[1] ZHE WANG,[1] TUAN GUO,[2] XUEHAO HU,[3] CHRISTOPHE CAUCHETEUR,[3,5] KAIWEI LI,[1,6] LEI REN,[1,4,7] AND LUQUAN REN[1,4]

[1]*Key Laboratory of Bionic Engineering (Ministry of Education), Jilin University, Changchun 130022, China*
[2]*Institute of Photonics Technology, Jinan University, Guangzhou 510632, China*
[3]*Department of Electromagnetism and Telecommunication, University of Mons, Boulevard Dolez 31, Mons 7000, Belgium*
[4]*Institute of Structured and Architected Materials, Liaoning Academy of Materials, Shenyang 110167, China*
[5]*christophe.caucheteur@umons.ac.be*
[6]*kaiwei_li@jlu.edu.cn*
[7]*lren@jlu.edu.cn*
[†]These authors contributed equally to this work.

Abstract: Stretchable optical fibers are emerging as a promising platform for wearable sensing applications, owing to their exceptional flexibility, high sensitivity, and inherent immunity to electromagnetic interference. Although current research primarily concentrates on conventional step-index configurations, microstructured optical fibers (MOFs) with precisely engineered architectures offer unprecedented design flexibility and functional versatility. Nevertheless, the fabrication of such advanced fiber structures poses significant technical challenges. This study introduces a demonstration of an elastomeric suspended-core MOF fabricated using styrene-ethylene-butylene-styrene (SEBS) through the preform-to-fiber thermal drawing process, achieving precise geometrical and dimensional control of the fiber structure. The fabricated fiber demonstrates remarkable performance characteristics, including low optical transmission loss (0.0621 dB/cm at 550 nm wavelength), mechanical robustness sustaining up to 500% strain, and superior optomechanical sensitivity under both normal pressure (0–10 N) and bending deformation (0°–90°). These attributes collectively validate its suitability for advanced wearable sensing applications. As a proof of concept, we demonstrate the elastic MOF's versatile applications across three domains: (1) robotic tactile sensing that discriminates surface textures via characteristic light attenuation, (2) high-accuracy data gloves for finger joint flexion tracking in gesture recognition, and (3) real-time respiratory monitoring with reliable breathing rate detection. The integration of SEBS-based elastomeric properties with enhanced optomechanical responsiveness creates a multifunctional platform for next-generation optical sensors in intelligent robotics, human-machine interfaces, and biomedical monitoring systems.

1. Introduction

The demand for wearable sensing has surged in fields such as intelligent robotics, human-machine interaction, and health monitoring, with the core challenge being the achievement of compatibility between high-fidelity mechanical signal acquisition and intrinsic compliance. Traditional electronic sensors are limited by issues such as electromagnetic interference, rigid circuitry, and power supply constraints [1,2]. In contrast, optical fiber sensing technology has emerged as an ideal alternative due to its immunity to interference, capability for distributed measurement, and

#576098 https://doi.org/10.1364/OE.576098
Journal © 2025 Received 15 Aug 2025; revised 19 Sep 2025; accepted 22 Sep 2025; published 30 Sep 2025

Optics EXPRESS

passive operation [3,4]. Particularly, elastomeric polymer optical fibers (POFs), which possess intrinsic mechanical flexibility, stretchability, and robustness while offering high sensitivity to mechanical deformation and excellent conformability to complex morphology surfaces, are attractive for intelligent wearable sensing systems [5].

In recent years, flexible and elastic optical fibers with extreme deformation capability and high sensitivity to mechanical stimuli and temperature have witnessed a flourishing development. The Seok-Hyun Yun group first developed a stretchable optical fiber made of hydrogel by the mold casting method. These optical fibers show good biocompatibility and can endure stretch up to 120%, which is beyond traditional rigid optical fibers [6,7]. Besides, silicone rubbers with good optical transparency are also employed for fabricating stretchable optical fibers via the mold casting method [8,9]. The good mechanical flexibility and extreme strain sensing ability make these fibers suitable for wearable body motion monitoring [9,10], physiological signal monitoring [11], and tactile sensing [8]. More importantly, doping the fiber core with functional dyes or nanomaterials, as well as inscribing Bragg gratings into the fiber core, can endow the fiber with the ability for temperature measurement [12,13], distributed tactile sensing [14,15], and even multimodal capabilities [16–19]. Self-powered sensing [20] and self-healing stretchable optical fibers have also been demonstrated [21]. The mold casting method provides a flexible design of the geometry of the fiber and facilitates the doping of functional materials inside the fiber. However, it also faces limitations; these optical fibers are relatively large, with cross-sectional diameters typically in the millimeter range. They have a relatively simple structure, typically being step-index multimode fibers. Their manufacturing process relies on manual labor, resulting in low production volumes.

In parallel, researchers are trying to employ transparent thermal processable polymers like TPU and TPE as raw materials for the production of stretchable optical fibers. This technique enables the mass production of optical fibers with high consistency; the optical fibers produced have a finer diameter, making them suitable for wearable applications; and more importantly, optical fibers with sophisticated cross-section geometries can be fabricated. Super elastic multimode optical fibers have been successfully fabricated with TPE using the standard fiber drawing technique, and implemented for motion monitoring and tactile sensing [22–24]. Single-mode stretchable elastic optical fibers that can withstand stretching rates of 700% have also been fabricated [25]. These super-stretchable optical fibers show excellent performance for strain, bending, and pressure sensing.

To date, most reported stretchable optical fibers are based on the traditional step-index fiber design, which inherently limits their functionality and sensing performance. Rigid microstructure optical fibers with ingenious and complex cross-section designs offer unprecedented control over light propagation through engineered microstructures and have revolutionized photonic technologies in the last two decades [26,27]. Elastomer-based microstructured optical fibers will greatly expand design flexibility, enabling enhanced functionality and sensing performance, and providing a physical platform for the next generation of intelligent sensing systems. Such fibers would be more mechanically flexible than all solid optical fibers owing to the air holes running along the whole fiber length, would provide a much larger freedom for fiber design as light guidance could be realized in both hollow cores and solid cores with tight confinement, with the possibility for programming the mechanical properties distribution within the fiber cross-section, thus engineering the sensitivity to mechanical stimuli. Moreover, the air holes running parallel with the core provide a vacancy for integrating functional materials with the fiber core to provide versatile sensing capabilities. Preliminary studies on hollow core optical fibers with a simple cross-section design have been fabricated with elastomers through the fiber drawing technique [28–31]. However, the fiber geometry is difficult to maintain due to the low modulus, low viscosity, and high adhesiveness of elastomers under high temperatures. This poses challenges for fabricating stretchable microstructured optical fibers with complex geometries.

Optics EXPRESS

In this study, we propose and demonstrate the first stretchable SEBS-based flexible six-hole suspended core fiber (SCF), which is suitable for intelligent wearable sensing. The SCF is fabricated through thermal drawing with a high production rate and high uniformity. The SEBS SCF features a 120 μm diameter core surrounded by six holes that provide tight light confinement. It shows a low optical loss coefficient of 0.0621 dB/cm at 550 nm and a large elongation capacity exceeding 500%. The flexible SEBS SCF, with a low elastic modulus, is susceptible to external stimuli such as pressure and bending. More importantly, the absence of cladding material around the core allows it to move or deform more freely, making it suitable for wearable sensing. As a proof of concept, we integrated the flexible SCF onto the fingers of an adaptive manipulator to endow it with the ability for contact pressure measurement during object grasping. Then, we integrated the SCF fiber into a glove and demonstrated the ability to track finger gestures. The flexible SEBS SCF could also find other applications, such as health monitoring and motion tracking. Overall, this study demonstrates the first thermally drawn stretchable microstructure optical fiber and its capability for intelligent wearable sensing. In the future, we foresee various forms of stretchable microstructure special optical fibers emerging.

2. Design, fabrication and characterization

2.1. Fiber design and fabrication

The elastomeric SCF features a SEBS solid core surrounded by six air holes. The fabrication of the fiber involves two sequential processes: preform fabrication and thermal drawing. In the preform fabrication stage, a customized metal holder is used to position six Teflon rods, each measuring 6.0 ± 0.1 mm in diameter, into a hexagonal array inside a fused silica tube with an inner diameter of 34.0 ± 0.5 mm. This arrangement ensures highly uniform circumferential symmetry and consistent interstitial spacing throughout the mold assembly (Fig. 1(a)). The interstitial voids between the Teflon rods and the inner wall of the silica tube are then filled with SEBS copolymer pellets (Kraton G1657). This material is selected for its favorable mechanical properties, including a tensile strength of 23 MPa and a Shore A hardness of 47, which contribute to the flexibility and structural integrity of the final preform. Once packed, the entire mold assembly is transferred to a vacuum oven for thermal processing. The SEBS pellets are heated to 250 °C under vacuum to eliminate air bubbles and prevent oxidation. Under these conditions, the pellets soften, coalesce, and gradually form a homogeneous fiber preform through thermal fusion. After a dwell time of 12 hours to ensure complete integration of the material, the mold is cooled slowly to room temperature under a maintained vacuum to minimize thermal stress and avoid deformation. Finally, the solidified SEBS preform is carefully released from the mold, resulting in a structured soft polymer preform ready for subsequent processing.

The preform is then thermally drawn into fibers with desired diameters at a temperature of ~240°C using a low-temperature optical fiber drawing tower, as shown in Fig. 1(b). The thermal drawing process employs rigorously optimized feeding rates and drawing speeds to ensure repeatable, large-scale fabrication. Owing to SEBS's exceptional elastic properties, the fiber demonstrates an elongation capacity of over 500%, as shown in Fig. 1(c). The cross-section of the SCF is shown in Fig. 1(d), indicating the successful fabrication of the six-hole SEBS SCF. Figure 1(e) shows a bunch of fabricated stretchable SEBS SCF that is rolled around a capstan.

2.2. Characterization and sensing performance

We first characterized the optical transmission property of the fabricated stretchable suspended-core fiber. We conducted finite element simulations to analyze the modal field distribution of the suspended-core fiber. The stretchable SCF supports multiple modes with similar effective refractive indices, indicating tight confinement to guided light. The electric field distribution of four typical guided modes supported by the SCF modes with effective indexes of 1.492795

Optics EXPRESS

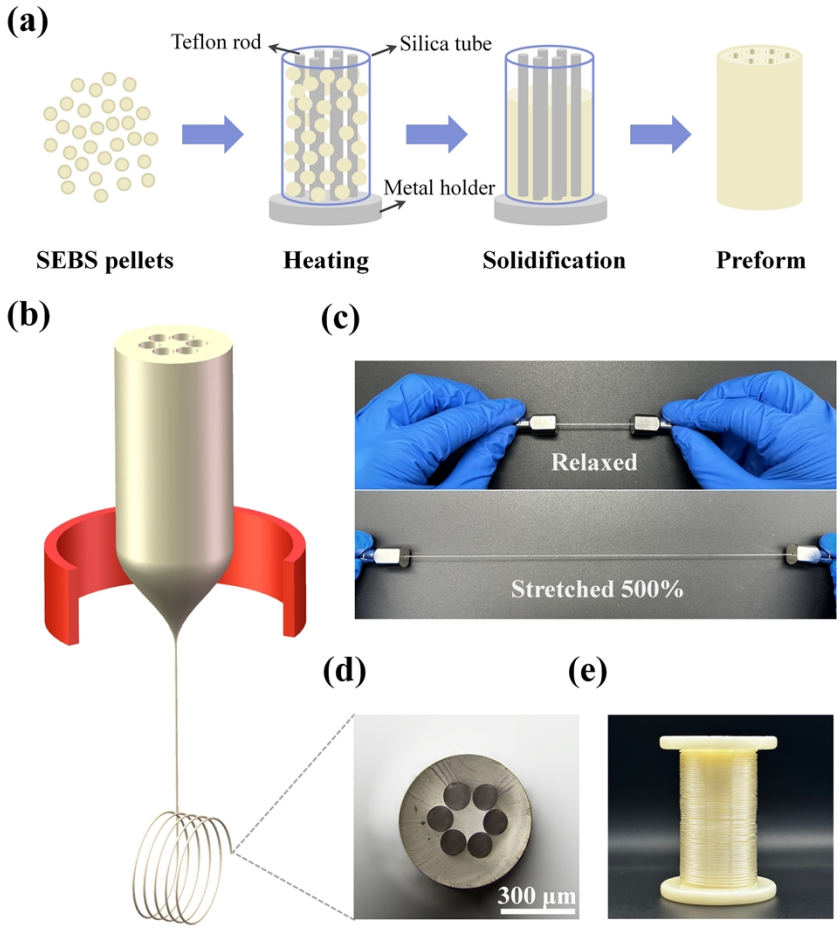

Fig. 1. Fabrication of the stretchable six-hole SEBS SCF. (a) Fabrication process of the fiber preform. (b) Schematic illustration of the thermal drawing process. (c) The SEBS SCF stretched to five times its original length. (d) Microscopic cross-sectional image of a 600 μm diameter SEBS SCF. (e) Batch production of the stretchable SCF.

(HE_{11}), 1.492789 (HE_{21}), 1.492781 (HE_{31}) and 1.492774 (HE_{41}) are shown in Fig. 2(a). For optical transmission measurements, the SEBS optical fiber is cut vertically using a brand-new blade to obtain a flat and smooth end facet. To eliminate the additional optical loss caused by fiber adaptors which induces deformation, we sealed the fiber in a Teflon tube with UV-curable adhesives to improve the stiffness of the fiber pigtail. Two pigtails were connected to a broadband white light source (Ideaoptics, HL2000) and a spectrometer (Ideaoptics, FX2000) via fiber adaptors.

The wavelength-dependent transmission loss was measured by the cut-back method, as incremental fiber lengths (25-40 cm) of the same fiber was cut to quantify the optical transmission performance, as shown in Fig. 2(b). Transmission spectra under incremental fiber lengths are shown in Fig. 2(c). Normalized transmission spectra for various fiber lengths are shown in Fig. 2(d). A linear regression analysis of the transmission data at a wavelength of 550 nm (Fig. 2(e)) yields a propagation loss coefficient of 0.0621 dB/cm ($R^2 = 99.7\%$).

We then characterized the sensing performance of the six-hole SEBS SCF towards normal force, bending, and stretching. Firstly, the SCF was mounted on a force testing setup comprising

Optics EXPRESS

a precision motorized translation stage, a force gauge, and a test probe. The optical response was measured as the applied force increased from 0 N to 10 N in increments of 1 N. As shown in Figs. 3(a) and 3(b), the transmission spectra and the normalized transmission intensity across the 500–750 nm range both decrease as the normal force increases. The evolution of the normalized intensity at a wavelength of 550 nm is shown in Fig. 3(c). It is evident that the slope of the curve is steep for small forces, gradually decreasing as the applied force increases, indicating a nonlinear response characteristic of the SEBS SCF.

For bending sensing, we mounted the SEBS SCF onto a bending testing apparatus and applied bending angles to the fiber from 0° to 90° in 10° increments. The bending radius is 7.5 mm. The transmission spectra and the normalized transmission spectra are presented in Figs. 3(d) and 3(e), respectively. It is clear that as the bending angle increases, the normalized transmission intensity across the 500–750 nm range decreases. The evolution of the normalized intensity at

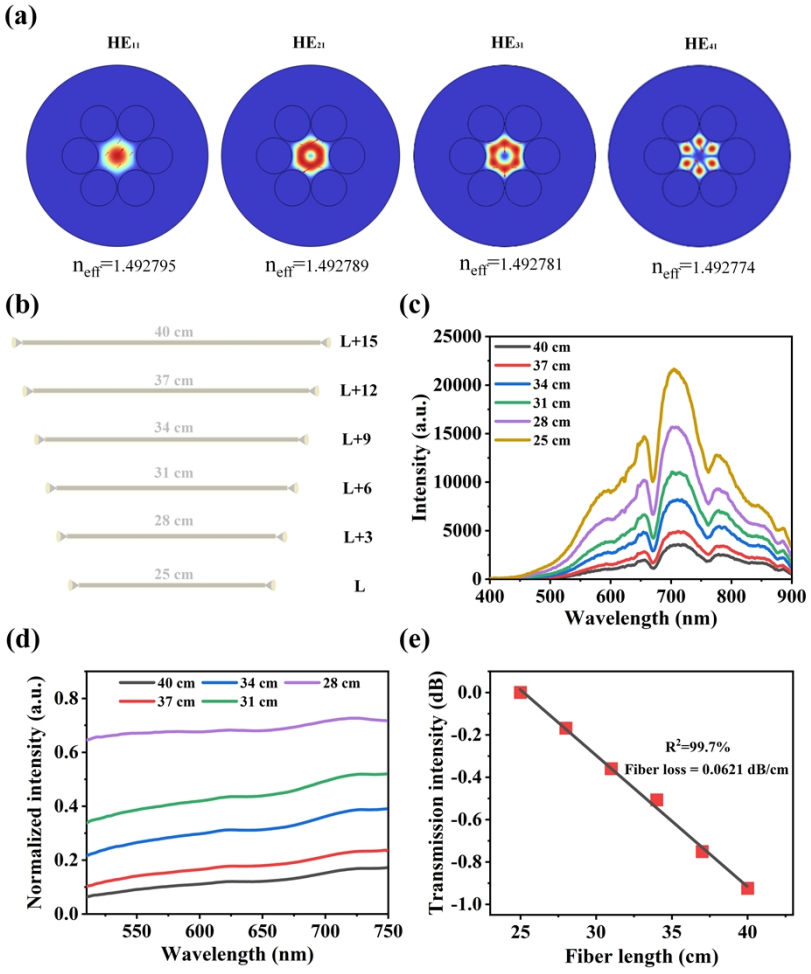

Fig. 2. Optical transmission characteristics of the six-hole SEBS SCFs. (a) Simulated electric field distribution of four typical core modes at a wavelength of 550 nm. (b) The cut-back method for measuring propagation loss with 3 cm length steps. (c) Transmission spectra of the SEBS SCF at varying lengths. (d) Normalized transmitted light intensity as a function of fiber length. (e) A linear relationship between transmitted light intensity and fiber length under tensile testing at a wavelength of 550 nm.

Optics EXPRESS

550 nm, shown in Fig. 3(d), demonstrates a linear response of the sensor to bending angle, with a coefficient of determination (R^2) of 99.9%.

To investigate the stretching sensitivity, the SEBS SCF was mounted on a stretching test apparatus, with the fiber subjected to strain elongation ranging from 0% to 50% in 5% increments. The transmission spectra and the normalized transmission spectra are shown in Figs. 3(g) and 3(h), respectively. As strain elongation increases, the normalized transmission intensity across the 500–750 nm range decreases. The evolution of the normalized intensity at 550 nm is shown in Fig. 3(i). It is evident that the slope of the curve is steep for small strain and decreases as the applied strain increases, indicating a nonlinear response characteristic of the SEBS SCF. We attribute the stretching induced optical loss to two factors. First, when the fiber is stretched, both its refractive index and diameter decrease, thereby weakening the fiber's ability to confine light, and leads to increased loss of guided modes, especially the higher-order mode. Simultaneously, as the fiber elongates, the intrinsic absorption loss of the SEBS optical fiber also increases. Please be noted that the fiber can endure elongation up to 500%. However, when the elongation exceeds 100%, the fiber becomes insensitive to stretching (see Fig. S3).

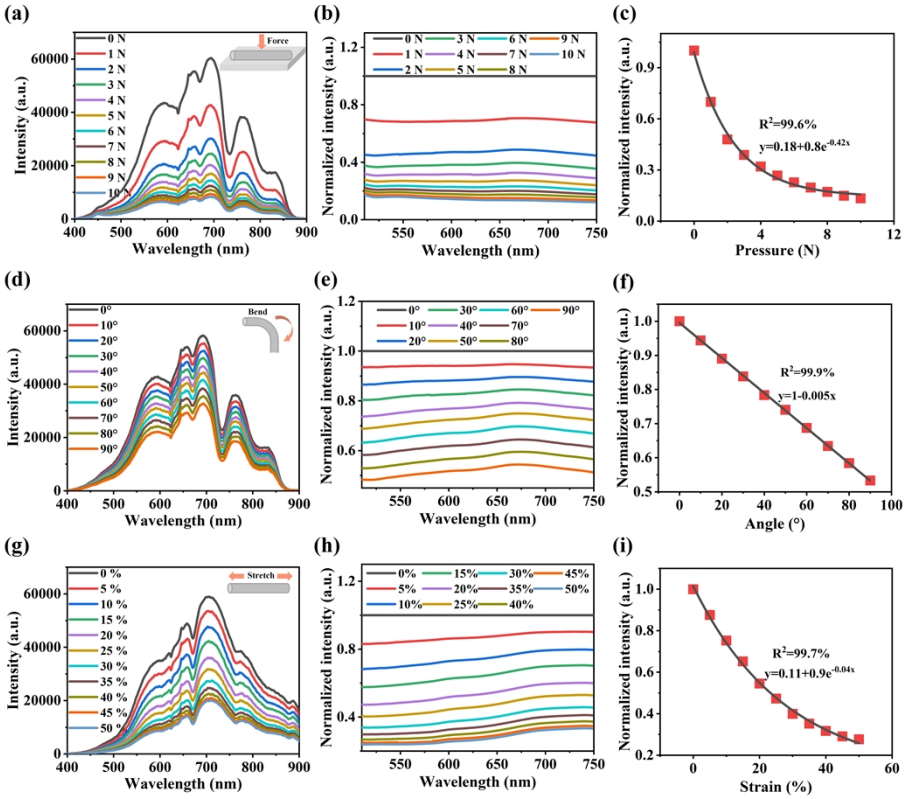

Fig. 3. Sensing performance of the flexible six-hole SCFs to pressure, bending, and stretching. (a) Transmission spectra of SCFs to pressure ranging from 0 to 10 N. (b) Normalized transmitted light intensity as a function of applied normal force. (c) Variation curve of transmitted light intensity during the pressure test. (d) Transmission spectra of SCFs under varying bending angles. (e) Normalized transmitted light intensity versus bending angle (0° to 90°). (f) Linear relationship between transmitted light intensity and bending angle obtained from the bending test. (g) Transmission spectra of SCFs under tensile strain (0% to 50%). (h) Normalized transmitted light intensity as a function of strain. (i) Variation curve of transmitted light intensity during the stretching test.

Optics EXPRESS

The robustness of the sensor was tested using a tensile testing machine. Figure S1 demonstrates the force sensing performance of the SCFs during 10,000 pressure cycles with forces ranging from 0.5 to 3 N. The results indicate excellent mechanical durability of the stretchable optical fiber. Its high mechanical stability and durability make it ideal for photonic mechanical sensing application. In addition, we also investigated the effect of ambient temperature on the performance of the fiber by taking the normal force sensing as an example. A section of the fiber was placed in a thermostat box for force measurement. Figure S2 shows the changes in normalized intensity at a wavelength of 550 nm for the SEBS SCF sensor in response to normal forces ranging from 0 to 10 N at different ambient temperatures (from 20°C to 40°C, with an increment of 10°C). The overlapping trends across different temperatures suggest that the sensor performs well within the temperature range of 20°C to 40°C.

3. Applications of the six-hole SEBS SCF for wearable sensing

3.1. Application in robotic tactile sensing

The flexible mechanical properties and excellent sensing performance of the proposed SEBS SCF in response to normal force make it a promising candidate for wearable tactile sensing applications. To demonstrate this, we integrated the SEBS SCF onto one finger of an adaptive two-finger gripper, highlighting its capability for tactile sensing. The SCF was molded into a U shape and integrated onto the fingertip of a two-finger adaptive robotic gripper (DH-robotics, AG-105-145). A schematic diagram of the gripper, with one finger equipped with the SEBS SCF, is shown in Fig. 4(a). One end of the fiber is connected to a light source, while the other end is linked to a miniature spectrometer to collect the optical signal. The application relies on monitoring the intensity change of transmitted light when the fiber sensor-equipped adaptive gripper grasps different objects.

When an object is grasped, the robotic hand induces lateral compression on the fiber, leading to attenuation in the transmitted light intensity. We monitored the transmission spectra in real-time as the gripper grasped various objects, including a paper cup, a charging plug, a pen holder, and a tape cutter. The normalized intensity of transmitted light decreased by different amounts (14%, 40%, 60%, 83%) for each object, as shown in Figs. 4(b)–4(e). We hypothesize that the observed attenuation is influenced by the mass, contact area, and surface roughness of the clamped objects, as these factors are known to affect mechanical interactions and surface properties. This further underscores the excellent tactile sensitivity of the fabricated optical fibers for interacting with various materials.

3.2. Application in hand gesture recognition

Based on the bending angle measurement capability of the SEBS SCF, we developed an optical data glove, with each finger equipped with a section of SEBS SCF. One end of each fiber was connected to an LED light source, while the other end was linked to a linear charge-coupled device (LCCD). As illustrated in Fig. 5(a), five sensing elements were strategically positioned along the finger phalanges (from distal to proximal) to capture the kinematics of the metacarpophalangeal (MCP) and proximal interphalangeal (PIP) joints. Figures 5(b)–5(e) display the recorded intensity fluctuations of the peak values for each six-hole SCF sensing unit. The real-time spectral analysis during gesture articulation (FIVE, OK, YEAH, GOOD) shows a strong correlation between joint flexion angles (0°-90°) and normalized intensity attenuation ($R^2 = 99.9\%$). This allows for the potential identification of the gesture being performed by analyzing the transmission spectra from the five fingers. This new approach could greatly contribute to gesture recognition sensing applications.

Optics EXPRESS

3.3. Application in respiratory monitoring

Finally, we demonstrate the capability of the fabricated SEBS SCF for wearable human physiological signal monitoring, using the respiration rate as an example. We integrated the SEBS SCF into a stretchable chest strap. One end of the fiber was connected to a miniaturized LED light source, while the other end was linked to a portable optical power meter. Sketch illustrations of the chest strap and a subject wearing the strap around the chest are shown in Fig. 5(f). The

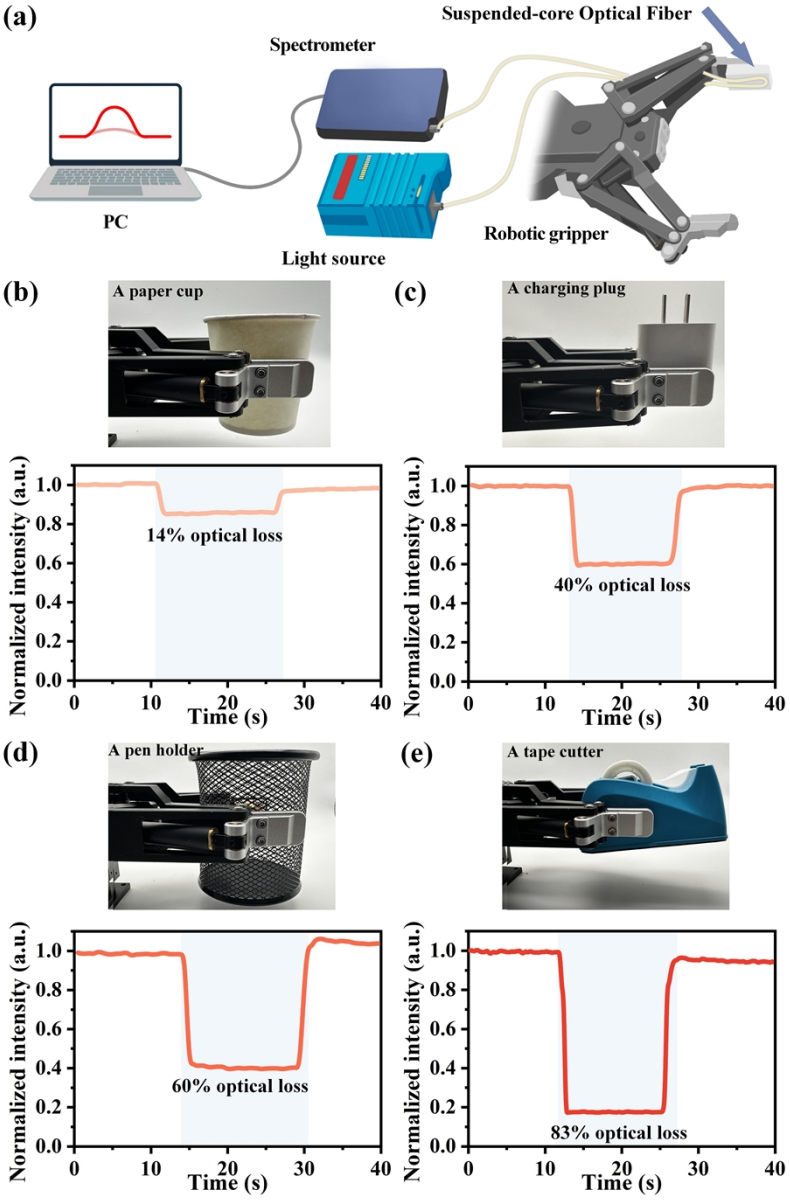

Fig. 4. Six-hole SEBS SCF for robotic tactile sensing. (a) The schematic diagram of the robotic gripper stress testing system. (b) Grasping and releasing a paper cup. (c) Grasping and releasing a charging plug. (d) Grasping and releasing a pen holder. (e) Grasping and releasing a tape cutter.

Optics EXPRESS

respiration rate was measured by monitoring the output optical power during the expansion and contraction of the thoracic cavity, which causes the chest strap and the stretchable SEBS SCF to stretch and release periodically during breathing. The sensor's output light intensity was recorded for the subject both at rest and immediately after completing a run. The variation of

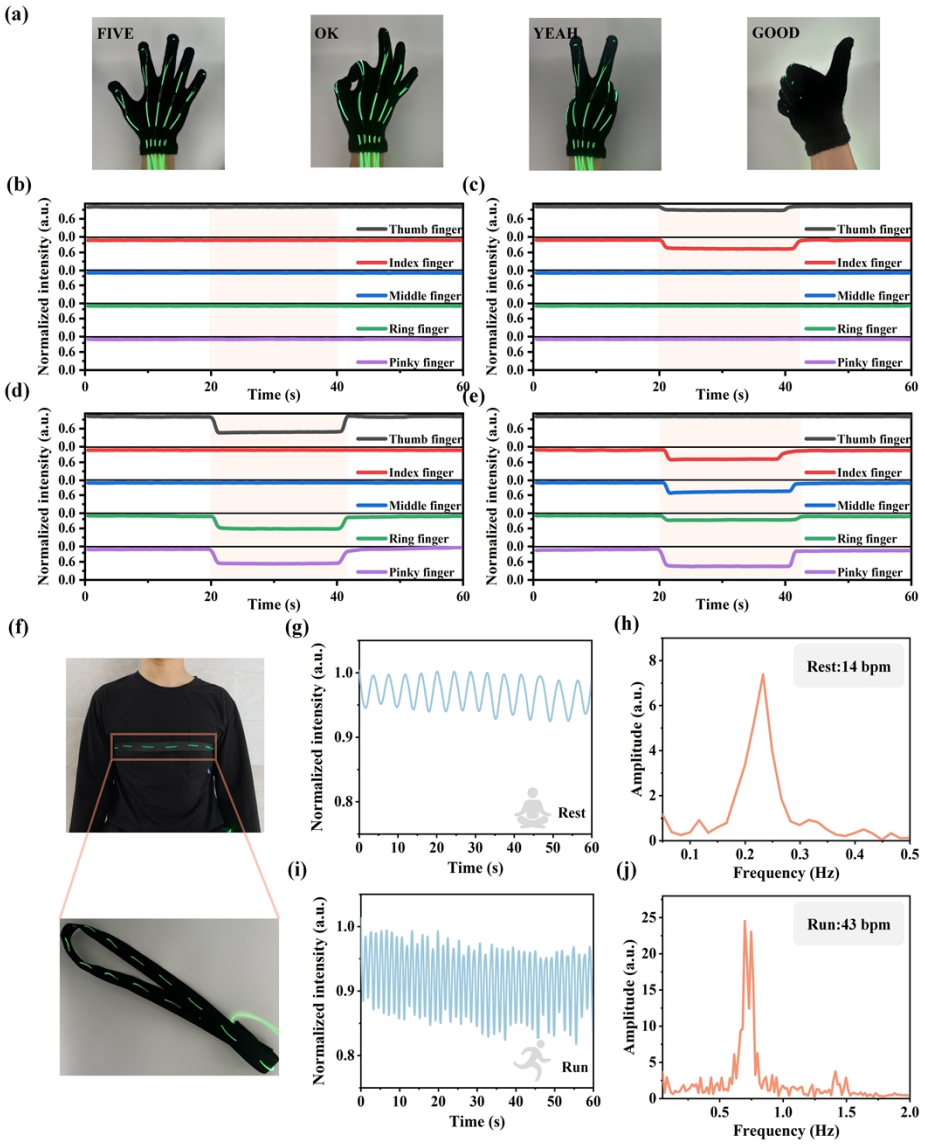

Fig. 5. Six-hole SEBS SCF for hand gesture recognition and wearable respiration rate monitoring. (a) Four gestures were made while wearing the data glove. (b) Optical intensity variation during the "FIVE" gesture. (c) Optical intensity variation during the "OK" gesture. (d) Optical intensity variation during the "YEAH" gesture. (e) Optical intensity variation during the "GOOD" gesture. (f) Schematic illustration of a subject wearing the chest strap integrated with a stretchable SEBS SCF segment. (g) Variation in normalized output light intensity while the subject is at rest. (h) FFT analysis of the real-time optical response during the resting state. (i) Variation in normalized output light intensity after the subject has completed running. (j) FFT analysis of the real-time optical response after running.

Optics EXPRESS

the normalized output light intensity for the subject in the resting state is shown in Fig. 5(g). It illustrates that the SEBS SCF is highly sensitive to breathing, with optical power decreasing and increasing periodically with the expansion and contraction of the thoracic cavity, respectively. A Fast Fourier Transform (FFT) of the measured real-time optical response reveals a respiration rate of 14 bpm for the subject at rest, as shown in Fig. 5(h). After running, the real-time response of the sensing fiber exhibits much denser and deeper periodic variations, as shown in Fig. 5(i). This indicates an increase in both respiration rate and depth after running. The FFT results show a respiration rate of 43 bpm, as depicted in Fig. 5(j). This case study demonstrates that our SEBS SCF is well-suited for wearable human physiological signal monitoring.

We have demonstrated the elastic SEBS SCF's sensing capability in three applications including robotic tactile sensing, high-accuracy data gloves for finger gesture recognition, and real-time respiratory monitoring. To further improve its stability and resistance to external interferences, we would retain a short section of the SEBS SCF for sensing, and use rigid plastic optical fibers for light guiding. Also, we would utilize highly stable miniaturized LED light sources so as to shorten the length of the light guiding section in our future study.

4. Conclusions

In conclusion, we have successfully fabricated the first soft and stretchable six-hole suspended-core optical fiber using the thermal drawing technique. This process enables precise geometric control and high production rates. The fiber, composed of the optically transparent elastomer SEBS, features a 120 μm solid core surrounded by six air holes. This unique structure synergistically combines low-loss light guidance with high optomechanical sensitivity. The inherent softness and outstanding elasticity of SEBS endow the fiber with excellent responsiveness to both pressure and strain, making it well-suited for wearable sensing applications. We validated its versatility through integration into three distinct platforms: a robotic tactile sensor, a wearable glove for gesture recognition, and chest straps for respiratory monitoring. These proof-of-concept demonstrations highlight the fiber's ability to detect subtle mechanical deformations with high sensitivity. This fiber architecture establishes a versatile platform for next-generation adaptive photonic devices, particularly in intelligent robotics and interactive biomedical technologies.

Funding. National Natural Science Foundation of China (52375288, 52405313); Jilin Provincial Key Research and Development Plan Project (20230101120JC); The Key Project of State Key Laboratory of Changchun City (23GZZ14); Fonds de la Recherche Scientifique (F.R.S.-FNRS) (Chargé de Recherches); The Open Fund of Guangdong Provincial Key Laboratory of Optical Fiber Sensing and Communication Technology.

Acknowledgments. The authors acknowledge the Funding from Fonds de la Recherche Scientifique (F.R.S.-FNRS) under the Postdoctoral Researcher grant (Chargé de Recherches) of Xuehao Hu and the Research Director Position of Christophe Caucheteur.

Disclosures. The authors declare no conflicts of interest.

Data availability. Data underlying the results presented in this paper are not publicly available at this time but may be obtained from the authors upon reasonable request.

Supplemental document. See Supplement 1 for supporting content.

References

1. H. C. Ates, P. Q. Nguyen, L. Gonzalez-Macia, *et al.*, "End-to-end design of wearable sensors," Nat. Rev. Mater. **7**(11), 887–907 (2022).
2. J. Tu, M. Wang, W. Li, *et al.*, "Electronic skins with multimodal sensing and perception," Soft Sci. **3**(3), 1–15 (2023).
3. J. N. Dash, X. Cheng, D. S. Gunawardena, *et al.*, "Rectangular single-mode polymer optical fiber for femtosecond laser inscription of FBGs," Photonics Res. **9**(10), 1931–1938 (2021).
4. Y. Mizuno, A. Theodosiou, K. Kalli, *et al.*, "Distributed polymer optical fiber sensors: A review and outlook," Photonics Res. **9**(9), 1719–1733 (2021).
5. Y. Wang, Y. Zhou, L. Qi, *et al.*, "Soft Optical Fibers for Biomedical and Wearable Technologies: Current Trends and Future Prospects," Adv. Funct. Mater. **Early View**, 2507712 (2025).
6. M. Choi, M. Humar, M. S. Kim, *et al.*, "Step-index optical fiber made of biocompatible hydrogels," Adv. Mater. **27**(27), 4081–4086 (2015).

Optics EXPRESS

7. J. Guo, X. Liu, N. Jiang, *et al.*, "Highly stretchable, strain sensing hydrogel optical fibers," Adv. Mater. **28**(46), 10244–10249 (2016).
8. H. Zhao, K. O'brien, S. Li, *et al.*, "Optoelectronically innervated soft prosthetic hand via stretchable optical waveguides," Sci. Robot. **1**(1), eaai7529 (2016).
9. J. Guo, M. Niu, and C. Yang, "Highly flexible and stretchable optical strain sensing for human motion detection," Optica **4**(10), 1285–1288 (2017).
10. C. K. Harnett, H. Zhao, and R. F. Shepherd, "Stretchable optical fibers: Threads for strain-sensitive textiles," Adv. Mater. Technol. **2**(9), 1700087 (2017).
11. J. Guo, B. Zhou, R. Zong, *et al.*, "Stretchable and highly sensitive optical strain sensors for human-activity monitoring and healthcare," ACS Appl. Mater. Interfaces **11**(37), 33589–33598 (2019).
12. J. Guo, B. Zhou, C. Yang, *et al.*, "Stretchable and temperature-sensitive polymer optical fibers for wearable health monitoring," Adv. Funct. Mater. **29**(33), 1902898 (2019).
13. E. Song, M. Chen, Z. Chen, *et al.*, "Mn^{2+}-activated dual-wavelength emitting materials toward wearable optical fibre temperature sensor," Nat. Commun. **13**(1), 2166 (2022).
14. H. Bai, S. Li, J. Barreiros, *et al.*, "Stretchable distributed fiber-optic sensors," Science **370**(6518), 848–852 (2020).
15. B. Hou, L. Yi, C. Li, *et al.*, "An interactive mouthguard based on mechanoluminescence-powered optical fibre sensors for bite-controlled device operation," Nat. Electron. **5**(10), 682–693 (2022).
16. J. Guo, B. Zhou, C. Yang, *et al.*, "Stretchable and upconversion-luminescent polymeric optical sensor for wearable multifunctional sensing," Opt. Lett. **44**(23), 5747–5750 (2019).
17. W. Bao, X. Li, F. Chen, *et al.*, "Bragg grating in a flexible and stretchable coreless polymer optical fiber," Opt. Lett. **47**(13), 3191–3194 (2022).
18. M. Chen, Y. He, H. Liang, *et al.*, "Stretchable and strain-decoupled fluorescent optical fiber sensor for body temperature and movement monitoring," ACS Photonics **9**(4), 1415–1424 (2022).
19. J. Guo, J. Tuo, J. Sun, *et al.*, "Stretchable multimodal photonic sensor for wearable multiparameter health monitoring," Adv. Mater. **37**(5), 2412322 (2025).
20. H. Liang, Y. He, M. Chen, *et al.*, "Self-powered stretchable mechanoluminescent optical fiber strain sensor," Adv. Intell. Syst. **3**(9), 2100035 (2021).
21. X. Wang, G. Chen, K. Zhang, *et al.*, "Self-healing multimodal flexible optoelectronic fiber sensors," Chem. Mater. **35**(3), 1345–1354 (2023).
22. Y. Qu, T. Nguyen-Dang, A. G. Page, *et al.*, "Superelastic multimaterial electronic and photonic fibers and devices via thermal drawing," Adv. Mater. **30**(27), 1707251 (2018).
23. Y. Zhang, X. Li, J. Kim, *et al.*, "Thermally drawn stretchable electrical and optical fiber sensors for multimodal extreme deformation sensing," Adv. Opt. Mater. **9**(6), 2001815 (2021).
24. J. Li, L. Chen, X. Yan, *et al.*, "Super-stretchable polymer optical fibers for robot finger posture and pressure recognition," J. Lightwave Technol. **43**(7), 3308–3315 (2025).
25. S. Shabahang, F. Clouser, F. Shabahang, *et al.*, "Single-mode, 700%-stretchable, elastic optical fibers made of thermoplastic elastomers," Adv. Opt. Mater. **9**(12), 2100270 (2021).
26. T. M. Monro and H. Ebendorff-Heidepriem, "Progress in microstructured optical fibers," Annu. Rev. Mater. Res. **36**(1), 467–495 (2006).
27. B. Li, Y. Zhao, Y. Zhang, *et al.*, "Functionalized micro structured optical fibers and devices for sensing applications: a review," J. Lightwave Technol. **39**(12), 3812–3823 (2021).
28. M. R. Kaysir, A. Stefani, R. Lwin, *et al.*, "Flexible optical fiber sensor based on polyurethane," in *Conference on Lasers and Electro-Optics Pacific Rim* (IEEE, 2017), pp. 1–2.
29. A. F. Runge, A. Stefani, R. Lwin, *et al.*, "Wearable polyurethane optical fiber based sensor for breathing monitoring," in *26th International Conference on Optical Fiber Sensors* (Optica Publishing Group, 2018), paper ThE75.
30. H. Banerjee, N. Bartolomei, and F. Sorin, "Soft microstructured optical fibers via thermal drawing," in *Advanced Photonics Congress* (Optica Publishing Group, 2022), paper SoM2H.1.
31. Y. Liu, Y. Wu, J. Li, *et al.*, "Super-Stretchable Liquid-Core Optical Fibers for Human Physiological Monitoring," J. Lightwave Technol. **43**(15), 7448–7454 (2025).